The Astrophysical Journal, 689:478–491, 2008 December 10
© 2008. The American Astronomical Society. All rights reserved. Printed in U.S.A.

A DYNAMICAL PERSPECTIVE ON ADDITIONAL PLANETS IN 55 CANCRI

Sean N. Raymond,[1,2] Rory Barnes,[3] and Noel Gorelick[4]

Received 2008 June 30; accepted 2008 August 17

ABSTRACT

Five planets are known to orbit the star 55 Cancri. The recently discovered planet f at 0.78 AU (Fischer et al.) is located at the inner edge of a previously identified stable zone that separates the three close-in planets from planet d at 5.9 AU. Here we map the stability of the orbital space between planets f and d using a suite of *n*-body integrations that include an additional, yet-to-be-discovered planet g with a radial velocity amplitude of 5 ms^{-1} (planet mass = 0.5–1.2 Saturn masses). We find a large stable zone extending from 0.9 to 3.8 AU at eccentricities below 0.4. For each system we quantify the probability of detecting planets b–f on their current orbits given perturbations from hypothetical planet g, in order to further constrain the mass and orbit of an additional planet. We find that large perturbations are associated with specific mean motion resonances (MMRs) with planets f and d. We show that two MMRs, 3f : 1g (the 1 : 3 MMR between planets g and f) and 4g : 1d cannot contain a planet g. The 2f : 1g MMR is unlikely to contain a planet more massive than $\sim 20\ M_\oplus$. The 3g : 1d and 5g : 2d MMRs could contain a resonant planet but the resonant location is strongly confined. The 3f : 2g, 2g : 1d, and 3g : 2d MMRs exert a stabilizing influence and could contain a resonant planet. Furthermore, we show that the stable zone may in fact contain 2–3 additional planets, if they are $\sim 50\ M_\oplus$ each. Finally, we show that any planets exterior to planet d must reside beyond 10 AU.

Subject headings: methods: *n*-body simulations — methods: statistical — planetary systems

Online material: color figures

1. INTRODUCTION

In a remarkable study, Fischer et al. (2008) have measured the orbits of five planets orbiting the star 55 Cancri, the most planets of any exoplanet system to date. The system contains two strongly interacting, near-resonant giant planets at 0.115 and 0.24 AU (Butler et al. 1997; Marcy et al. 2002), a "hot Neptune" at 0.038 AU (McArthur et al. 2004), a Jupiter analog at 5.9 AU (Marcy et al. 2002) and a newly discovered sub-Saturn-mass planet at 0.78 AU (Fischer et al. 2008). Table 1 lists the Fischer et al. self-consistent dynamical fit of the orbits of the five known planets in 55 Cancri.

The fast-paced nature of exoplanet discoveries can lead to interesting interactions between theory and observation. Prior to the discovery of planet 55 Cancri f, several groups had mapped out the region between planets c and d to determine the most likely location of additional planets. Most studies used massless test particles to probe the stable zone (Barnes & Raymond 2004, hereafter BR04; Jones et al. 2005; Rivera & Haghighipour 2007). Test particles are good proxies for small, Earth-sized planets because they simply react to the ambient gravitational field. However, they are not good substitutes for fully interacting, real planets. Thus, Raymond & Barnes (2005, hereafter RB05) mapped out this zone using Saturn-mass test planets. The stable zone from BR04 and RB05 extended from 0.7 to 3.2–3.4 AU, a region that includes the star's habitable zone (Raymond et al. 2006). The planet 55 Cnc f was discovered by Fischer et al. at the inner edge of that stable zone.

The "packed planetary systems" (PPS) hypothesis asserts that if a zone exists in which massive planets are dynamically stable, then that zone is likely to contain a massive planet (BR04; RB05; Raymond et al. 2006; Barnes et al. 2008). Although the idea behind the PPS hypothesis is not new (see, e.g., Laskar 1996), the large number of planetary systems being discovered around other stars allows PPS to be tested directly. Indeed, the ~1.4 Saturn mass planet HD 74156 d recently discovered by Bean et al. (2008) was located in the stable zone mapped out in BR04 and RB05, and with the approximate mass predicted by RB05 (Barnes et al. 2008). In addition, most of the first-discovered planetary systems are now known to be packed (Barnes et al. 2008), as well as ~85% of the known two-planet systems (Barnes & Greenberg 2007). The fact that 55 Cancri f lies within the stable zone identified in previous work (BR04; RB05) also supports PPS, especially since planets e through c are packed, i.e., no additional planets could exist between them. Several other planet predictions have been made and remain to be confirmed or refuted (see Barnes et al. 2008)—the most concrete outstanding prediction is for the system HD 38529 (see RB05).

Mean motion resonances (MMRs) are of great interest because they constrain theories of planet formation. Models of convergent migration in gaseous protoplanetary disks predict that planets should almost always be found in low-order MMRs and with low-amplitude resonant libration (Snellgrove et al. 2001; Lee & Peale 2002). This may even have been the case for the giant planets in our solar system (Morbidelli et al. 2007). On the other hand, planet-planet scattering can produce pairs of resonant planets in ~5% of unstable systems, but with large-amplitude libration and often in higher order MMRs (Raymond et al. 2008). Thus, understanding the frequency and character of MMRs in planetary systems is central to planet formation theory.

In the context of PPS, 55 Cancri is an important system as it contains many planets, but still appears to have a gap large enough to support more planets. Therefore, PPS makes a clear prediction that another planet must exist between known planets f and d. In this paper we add massive hypothetical planets to the system identified by Fischer et al. (2008) to determine which physical and orbital properties could still permit a stable planetary system. We focus our search on the "new" stable zone between

[1] Center for Astrophysics and Space Astronomy, University of Colorado, UCB 389, Boulder CO 80309-0389; raymond@lasp.colorado.edu.
[2] NASA Postdoctoral Program Fellow.
[3] Lunar and Planetary Laboratory, University of Arizona, Tucson, AZ.
[4] Google, Inc., 1600 Amphitheater Parkway, Mountain View, CA 94043.

TABLE 1
Self-Consistent Dynamical Fit of 55 Cancri (Fischer et al. 2008)

Planet	$M \sin i$ (M_J)	a (AU)	e	±	ϖ	T_{peri} (JD − 2,440,000)
e	0.024	0.038	0.263	0.06	156.5	7578.2159
b	0.84	0.115	0.016	0.01	164.0	7572.0307
c	0.17	0.241	0.053	0.052	57.4	7547.525
f	0.14	0.785	0.0002	0.2	205.6	7488.0149
d	3.92	5.9	0.063	0.03	162.7	6862.3081

planets f and d. We also show that certain dynamically stable configurations are unlikely to contain a planet because the large eccentricity oscillations induced in the known planets significantly reduce the probability of Fischer et al. having detected the known planets on their identified orbits, to within the observational errors. The orbital regions that perturb the known planets most strongly correlate with specific dynamical resonances, such that we can put meaningful constraints on the masses of planets in those resonances. Finally, we also use test particle simulations to map out the region of stability for additional planets beyond planet d, in the distant reaches of the planetary system.

2. METHODS

Our analysis consists of four parts; the methods used for each are described in this section. First, we map the stable zone between planets f and d using massive test planets—note that we use the term "test planets" to refer to massive, fully interacting planets. Our numerical methods are described in § 2.1.1. Second, we use massless test particles to map the stability of orbits exterior to planet d, as described in § 2.1.2. Third, we use the same technique to map several mean motion resonances in the stable region. A simple overview of resonant theory is presented in § 2.2. Finally, we use a quantity called the FTD—defined in § 2.3—to evaluate the probability of detecting stable test planets.

2.1. *Numerical Methods*

2.1.1. *Massive Test Planets*

We performed 2622 six-planet integrations of the 55 Cancri planetary system which include an additional hypothetical planet g located between known planets f and d. In each case, the known planets began on orbits from Table 1 including randomly assigned mutual inclinations of less than 1°. Planet g was placed from 0.85 to 5.0 AU in increments of 0.03 AU and with eccentricity between 0.0 and 0.6 in increments of 0.033. The mass of planet g was chosen to induce a reflex velocity of 5 m s^{-1} in the 0.92 $M_\odot$ host star (Valenti & Fischer 2005): its mass was varied continuously from ∼50 $M_\oplus$ inside 1 AU to 120 $M_\oplus$ at 5 AU. Orbital angles of the planets g were chosen at random. The system was integrated for 10 Myr using the symplectic integrator Mercury (Chambers 1999), based on the Wisdom-Holman mapping (Wisdom & Holman 1991) We used a 0.1 day time step and all simulations conserved energy to better than 1 part in 10^6. Integrations were stopped when they either reached 10 Myr or if a close encounter occurred between any two planets such that their Hill radii overlapped.

Although 10 Myr is much less than the typical ages of extrasolar planetary systems (∼Gyr), for a survey of this magnitude it is impractical to simulate each case for Gyr. Previous *N*-body integrations of extrasolar planets have shown that 10^6 orbits is sufficient to identify ∼99% of unstable configurations (Barnes & Quinn 2004). Moreover, *N*-body models of stability boundaries are consistent with alternative methods, such as the "mean exponential growth of nearby orbits" (MEGNO; Cincotta & Simó 2000) or fast Lyapunov indicators (Froeschlé et al. 1997; Sándor et al. 2007). For example, 1 Myr *N*-body integrations of the 2 : 1 resonant pair in HD 82943 (Barnes & Quinn 2004) identified a stability boundary that is very close to that of a MEGNO calculation (Goździewski & Maciejewski 2001). More recently, Barnes & Greenberg (2006), using 1 Myr *N*-body integrations, derived a quantitative relationship between the Hill and Lagrange stability boundaries for the nonresonant planets in HD 12661 that is nearly identical to a MEGNO study (Šidlichovský & Gerlach 2008). Therefore, for both resonant and nonresonant cases, 10^7 yr integrations provide a realistic measurement of stability boundaries.

In § 4 we performed several thousand additional integrations but with hypothetical planet g in or near specific mean motion resonances (MMRs) with planet f or d. In each case we aligned planet g's longitude of pericenter ϖ and time of perihelion with either planet f or d unless otherwise noted. Small mutual inclinations (<1°) between the two planets were included, with random nodal angles. Each set of simulations focused on a given MMR and included test planets of fixed mass with a range of orbital parameters designed to cover the MMR. The number of simulations ranged from 30 (4g : 1d) to >1100 (2g : 1d) simulations per set. Planet g's mass was constant in each set of simulations but varied by a factor of 2–3 between sets from the maximum value (RV = 5 ms^{-1}) down to 10–40 $M_\oplus$. We performed 2–3 sets for each MMR.

Our results are clearly sensitive to the assumed "true" orbits and masses of planets b–f. For this work we have adopted Fischer et al.'s (2008) self-consistent dynamical fit, but the observational uncertainties remain large. However, the locations of the MMRs in question scale simply with the semimajor axis of planet d or f. The strength of these MMRs depends on the mass and eccentricity of planets d or f (e.g., Murray & Dermott 1999). The eccentricity of planet d is relatively well known, while that of planet f is weakly constrained. Thus, the system parameters that could affect our results are e_f, M_d, and M_f. Since we assumed a small value of e_f, any increase would affect the strength of the 3f : 2g, 2f : 1g, and 3f : 1g MMRs. If M_f and M_d increase due to a determination of the system's observed inclination, then all the resonances we studied will increase in strength. This will tend to destabilize planets and also increase the size of chaotic zones. Thus, our results are likely to be "lower limits" in terms of the strength of resonances. Despite these potential issues, our simulations provide a realistic picture of the (in)stability of each MMR.

2.1.2. *Massless Test Particles*

To give a more complete view of the planetary system, we also tested the stability of planets exterior to planet d (5.9 AU). We used massless test particles for these simulations because of their smaller computational expense. Test particles were spaced by 0.01 AU from 6 to 30 AU (2401 total particles), and were given zero eccentricity, zero inclination orbits. All five known planets were included with orbits from Table 1, including randomly assigned

inclinations of less than 1°. As in previous runs, we used the Mercury hybrid integrator (Chambers 1999) with a 0.1 day time step and integrated the system for 10 Myr.

2.2. *Theory of Mean Motion Resonances* (*MMRs*)

For mean motion resonance $p + q : p$, the resonant arguments θ_i (also called "resonant angles") are of the form

$$\theta_{1,2} = (p + q)\lambda_1 - p\lambda_2 - q\varpi_{1,2}, \quad (1)$$

where λ are mean longitudes, ϖ are longitudes of pericenter, and subscripts 1 and 2 refer to the inner and outer planet, respectively (e.g., Murray & Dermott 1999). Resonant arguments effectively measure the angle between the two planets at the conjunction point—if any argument librates rather than circulates, then the planets are in mean motion resonance. In fact, the bulk of resonant configurations are characterized by only one librating resonant argument (Michtchenko et al. 2008). In general, libration occurs around equilibrium angles of zero or 180°, but any angle can serve as the equilibrium. Different resonances have different quantities of resonant arguments, involving various permutations of the final terms in equation (1). For example, the 2 : 1 MMR ($q = 1, p = 1$) has two resonant arguments, and the 3 : 1 MMR ($q = 2, p = 1$) has three arguments:

$$\theta_1 = 3\lambda_1 - \lambda_2 - 2\varpi_1, \quad \theta_2 = 3\lambda_1 - \lambda_2 - 2\varpi_2,$$
$$\theta_3 = 3\lambda_1 - \lambda_2 - (\varpi_1 + \varpi_2). \quad (2)$$

In § 4 we focus on the possibility of a hypothetical planet g existing in several MMRs in the stable zone between planets f and d. We measure the behavior of planets in and near resonance using the appropriate resonant arguments, as well as the relative apsidal orientation, i.e., $\varpi_g - \varpi_{d,f}$.

2.3. *The FTD Value* (*"Fraction of Time on Detected Orbits"*)

We have developed a simple quantity to constrain the location of hypothetical planet g beyond a simple stability criterion. To do this, we consider the observational constraints on the orbits of known planets b–f (1 σ error bars from Fischer et al. (2008) are listed in Table 1). A stable test planet can induce large oscillations in the eccentricities of the observed planets. Systems undergoing large eccentricity oscillations can be stable indefinitely as long as their orbits remain sufficiently separated (Marchal & Bozis 1982; Gladman 1993; Barnes & Greenberg 2006, 2007). However, systems with large eccentricity oscillations are less likely to be observed in a specific eccentricity range, especially with all planets having relatively small eccentricities, as is the case for 55 Cancri. The probability that a hypothetical planet g can exist on a given orbit is related to the fraction of time that known planets b–f are on their current orbits, to within the observational error bars. We call this quantity the FTD ("fraction of time on detected orbits"). If the FTD is small, then it is unlikely for planet g to exist on that orbit, because perturbations from planet g have decreased the probability of the *already made* detection of planets b–f. However, if the FTD is close to 1, then planet g does not significantly affect the likelihood of detecting the other planets and therefore hypothetical planet could exist on the given orbit. We have calibrated the FTD to have a value of unity for the known five-planet system (with no planet g). To perform this calibration, we artificially increased the observational error of planet c from 0.008 to 0.013. This was necessary simply because the evolution of the five known planets causes planet c's eccentricity to oscillate with an amplitude that is larger than its observational uncertainty, such that the FTD of the five-planet system is ~0.65. Thus, we calibrate by artificially increasing the uncertainty to roughly match the oscillation amplitude. As the region of interest lies between planets f and d, low FTD values are virtually always due to increases in the eccentricities of planets f or d. The small change we made to the error of planet c does not affect our results, and different methods for calibrating the FTD yield similar values. The FTD value therefore represents a quantity that measures the perturbations of a hypothetical planet g on the detectability of observed planets b–f, normalized to the amplitude of the self-induced perturbations of planets b–f.

To summarize, regions of high FTD (white in upcoming figures) represent orbits of planet g which are consistent with current observations of the system. Regions of low FTD (blue or black) represent orbits which significantly decrease the probability of detecting planets b–f on their observed orbits. Thus, we do not expect an additional planet to exist in regions with low FTD. Our confidence in this assertion scales with the FTD value itself (see color bar in upcoming figures). We allow FTD value to be below 50%, although this choice is arbitrary and much of the dynamical structure of the stable region is revealed at FTD values above 0.5. Note that all regions that have an FTD value are dynamically stable for our 10 Myr integration.

3. THE STABLE ZONE BETWEEN PLANETS f AND d

Figure 1 shows the stable zone between planets f and d: 984 of the 2622 simulations were stable (37.5%). Hatched areas indicate unstable regions, white and gray/blue indicate stable zones. The inner edge of the stable zone is defined by orbits that approach within a critical distance of planet f (the dashed line denotes orbits that cross those of planets f or d). The outer regions of the stable zone are carved by resonances with the ~4 Jupiter-mass planet d. Virtually no stable regions exist exterior to the 2 : 1 mean motion resonance (MMR) with planet d at 3.7 AU, except for the 3 : 2 MMR at ~4.5 AU (not all test planets at 4.5 AU in Figure 1 are in resonance because angles were chosen randomly). Note that the outer boundary of the stable zone is more distant than the one mapped in RB05 and BR04—this is due to a decrease in the best-fit eccentricity of planet d, reducing the strength of its secular and resonant perturbations. For a given semimajor axis and eccentricity of test planet g, the blue scale of Figure 1 represents the FTD, i.e., the probability of detecting known planets b–f on their current orbits (see color bar). The dark observationally unlikely areas do not fall at random, but are associated with specific dynamical structures within the stable zone. The wide, dark band from 1.3 to 2 AU with $e \sim 0.2$–0.4 are orbits for which secular perturbations from planet g increase the eccentricity of planet f above 0.2. The wide dark dip from 2 to 2.4 AU at smaller eccentricities is associated with a secular resonance between planets f and g which also increases the eccentricity of planet f above its observational limit. All other observationally unlikely (i.e., low FTD, dark) regions are caused by MMRs with planets f or d, although some are not clearly resolved in Figure 1 because the resonance is narrow. There is clearly room in between planets f and c for an additional planet; in § 5 we explore the possibility that multiple companions might lie in this zone.

4. MEAN MOTION RESONANCES (MMRs)

We performed extensive additional simulations to test the stability of parameter space in the vicinity of eight resonances in the stable zone—2g : 3f (the 2 : 3 MMR between planets g and f), 1g : 2f, 1g : 3f, 4g : 1d, 3g : 1d, 5g : 2d, 2g : 1d, and 3g : 2d. The location of these resonances is shown in Figure 1 and listed in Table 2. Based on our results, we divide the eight MMRs into three categories: stable, unstable, and neutral resonances. A stable

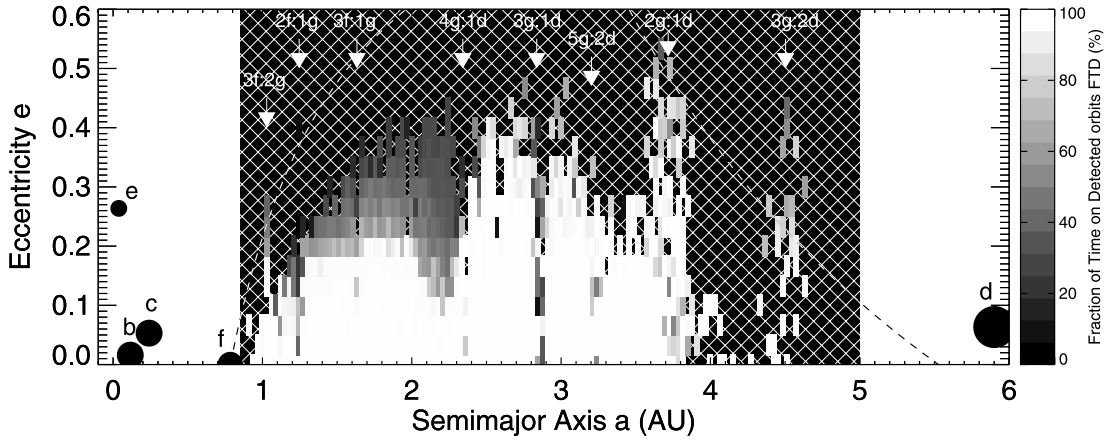

FIG. 1.—Stable zone between planets f and d. White regions represent the orbital elements of simulations with an additional test planet that were stable for 10 Myr. Black regions were unstable. Gray regions were stable but are unlikely to contain an additional planet because perturbations of the other planets' orbits were too strong (see text for discussion). Planets b through f are labeled. [*See the electronic edition of the Journal for a color version of this figure.*]

MMR effectively stabilizes a given region against secular perturbations (i.e., long-term gravitational perturbations far from resonance; see, e.g., Murray & Dermott 1999). For example, as seen in Figure 1, there are locations associated with the 3g : 2d MMR at ~4.5 AU that, although they cross planet d's orbit, are stable for long timescales. Conversely, an unstable resonance destabilizes a region that would be stable under just secular perturbations. For example, the region at 2.8–3.0 AU is well shielded from secular perturbations, but the 3g : 1d MMR at 2.88 AU causes a large swath of nearby orbits to be unstable. A neutral resonance is one where a region would be stable under secular perturbations, and remains stable with the resonance. Although the stability of test planets is not strongly affected by these MMRs, FTD values can be strongly affected, which in turn affect the likelihood of detecting a planet in a neutral resonance.

We see general similarities between different resonances. In many cases there exists a small region that can undergo resonant libration—that region is usually confined in a_g, e_g, and M_g (the mass of planet g) space. Planets in this region undergo regular eccentricity oscillations such that their FTD values are usually quite high, i.e., a planet can exist in that zone. Just outside a resonant region there often exists a chaotic zone in which planets may undergo temporary capture into the resonance. These zones are characterized by large irregular eccentricity variations that can eventually lead to close encounters and dynamical instability. The instability timescale is shorter for smaller M_g such that these chaotic zones are more populated for large M_g. However, given the relatively short 10 Myr duration of our integrations, we suspect that these chaotic zones would be cleared out in the system lifetime. We also found that stable zones with apsidal libration often exist close to the resonance.

4.1. *Stable Resonances*—3f : 2g, 2g : 1d, *and* 3g : 2d

4.1.1. *The 3f : 2g MMR*

The 3f : 2g MMR is located from 1.02 to 1.04 AU. Figure 2 shows the outcome of 136 simulations with planet g in the resonant region, formatted as in Figure 1. Two stable peaks extend above the collision line with planet f, at 1.024 and 1.034—1.039 AU. To avoid a close encounter and maintain dynamical stability, these planets must be in the 3 : 2 MMR. Indeed, the resonance provides a protection mechanism to maintain stability despite crossing orbits. The resonant dynamics prevents close encounters from happening by phasing orbital angles in various ways (see § 3 of Marzari et al. 2006)—this is also the case for the 2g : 1d and 3gL2d MMRs. As expected, we find that all planets on the two peaks above the collision line undergo resonant libration of $\theta_1 = 3\lambda_g - 2\lambda_f - \varpi_g$ about 180°. In the peak at 1.034 AU, resonant orbits extend down to zero eccentricity. However, the resonance associated with the peak at 1.024 AU extends down to $e_g \sim 0.05$. Below that limit and for the rest of the nearby, low-eccentricity stable zone, test planets are not in resonance with planet f.

Figure 3 shows the evolution of a simulation above the collision line with planet f. Libration of θ_1 about 180° is apparent. In

TABLE 2
CONSTRAINTS ON RESONANT PLANETS

Resonance	Location (AU)	Comments
2f : 3g	1.02–1.04	Resonant fingers at 1.024 and 1.034-1.039 AU. High FTD in fingers at $e_g \lesssim 0.2$.
1f : 2g	1.23–1.26	For $M_g = 30$ or 60 $M_\oplus$ resonance is limited to tiny region with very small FTD. Upper limit on resonant planet is ~20 $M_\oplus$.
1f : 3g	1.63	No stable planets show resonant libration.
4g : 1d	2.35	No stable planets show resonant libration.
3g : 1d	2.85–2.89	High-FTD resonant island exists at $a_g = 2.86$–2.89 AU and $e_g \leq 0.06$. Island of apsidal libration at $a_g = 2.85$–2.88 AU and $e_g = 0.15$–0.2.
3g : 1d anti[a]	2.85–2.89	High-FTD resonant island exists at $a_g = 2.86$–2.89 AU and $e_g \leq 0.01$. No island of apsidal libration.
5g : 2d	3.20	High-FTD resonant island at $a_g = 3.20$–3.225 AU and $e_g = 0.25$–0.4.
2g : 1d	3.7–3.8	Resonant island at $a_g = 3.6$–3.85 AU and $e_g \lesssim 0.6$.
3g : 2d	4.4–4.6	Resonant island $a_g = 4.4$–4.6 AU and $e_g = 0.1$–0.4.

[a] 3 : 1 MMR with planet d with antialigned longitudes of pericenter.

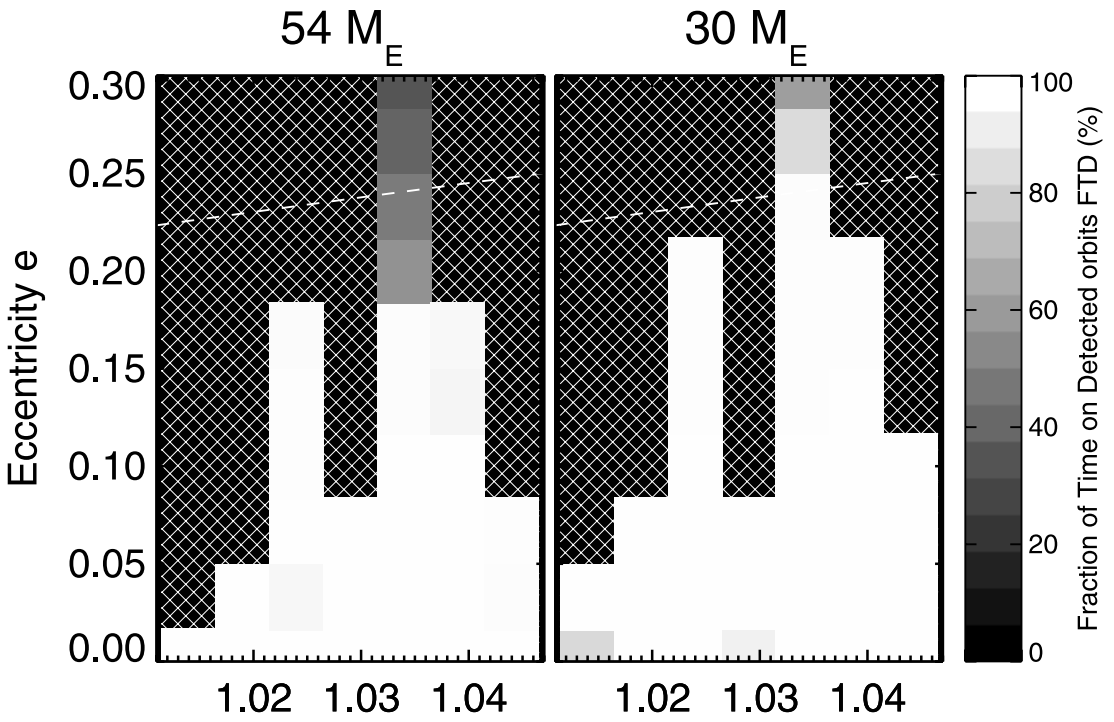

FIG. 2.—Stability and FTD of test planets in and near the 2 : 3 MMR with planet f (also called 2f : 3g), labeled by the test planet mass. The dashed line represents the collision line with planet f. Formatted as in Fig. 1. [*See the electronic edition of the Journal for a color version of this figure*.]

contrast, $\varpi_g - \varpi_f$ and θ_2 are preferentially found near 0° but they do occasionally circulate. If all three angles were librating then the system would be in apsidal corotation resonance; Beaugé & Michtchenko 2003; Ferraz-Mello et al. 2003). The eccentricities of planets g and f oscillate out of phase with amplitudes of $\sim$0.3. Note that e_f therefore exceeds the limits of its observational uncertainty, since its nominal current value is $\sim$0 with an uncertainty of 0.2. Thus, this simulation has a low FTD value of 0.335.

FTD values for test planets above the collision line are smaller for larger values of M_g. However, more than half of resonant configurations have very high FTD values. Therefore, a planet as massive as 54 $M_\oplus$ could reside in the 3f : 2g MMR, but only at low eccentricity ($e_g \lesssim 0.2$).

4.1.2. *The* 2g : 1d *MMR*

The 2 : 1 MMR with planet d (2g : 1d) is a wide, stable resonance located from 3.6 to 3.85 AU, and in some cases extending above the collision line with planet d. Figure 4 shows the outcomes of our integrations near the resonance. There is a peak of stability from 3.6 to 3.9 AU, and a sharp cliff of instability for $a_g > 3.9$ AU. The height of the peak depends on M_g: the stable region extends to higher e for more massive planets. The majority of the stable region in Figure 4 participates in the 2g : 1d MMR, i.e., at least one resonant argument librates. However, the behavior of different resonant arguments varies with M_g Figure 5 shows the stable zone from Figure 4 color-coded by which angle is librating ($\theta_1 = 2\lambda_d - \lambda_g\varpi_g$ and $\theta_2 = 2\lambda_d - \lambda_g - \varpi_d$). The libration of θ_1 is widespread and covers a large area. In contrast, θ_2 librates only in cases with $M_g = 100\ M_\oplus$, at the center of the resonance, right on the collision line with planet d. In cases where θ_2 librates, θ_1 and $\varpi_g - \varpi_d$ also librate in a configuration known as an apsidal corotation resonance. For lower M_g, the apsidal corotation resonance is apparent only in a few cases for $M_g = 50\ M_\oplus$. It is interesting that the small island of θ_2 libration for $M_g = 100\ M_\oplus$ has very high FTD values, while surrounding areas, while still in the resonance, have far lower FTD values (Fig. 4). These high FTD areas are shifted to slightly higher e_g for $M_g = 50\ M_\oplus$ and are in fact unstable for $M_g = 20\ M_\oplus$. If a planet g exists in the 2g : 1d MMR, then it must be localized in both mass and orbital parameter space. For large M_g, the planet could be either right on the collision line with planet d at $a_g \sim 3.73$ AU and $e_g \sim 0.5$, or in

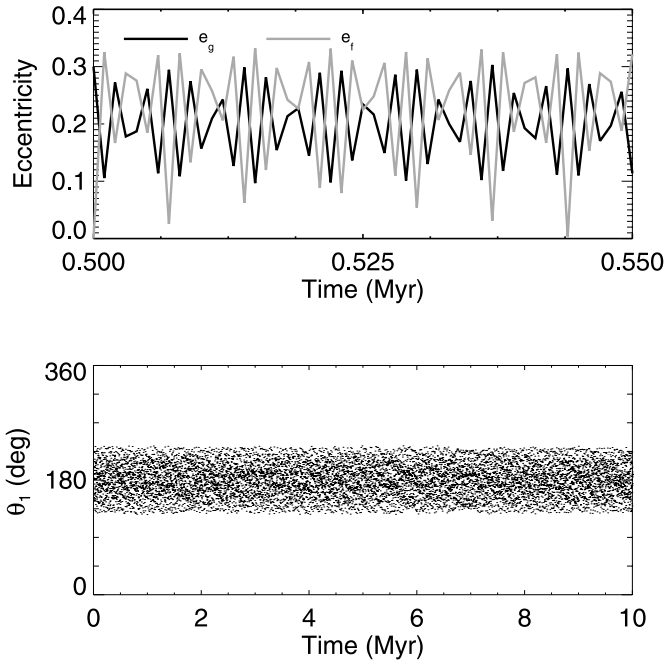

FIG. 3.—Evolution of a stable simulation in the 3f : 2g MMR, with planet g starting at 1.033 AU with $e_g = 0.3$. *Top*: Eccentricities of planets g (*black*) and *f* (*gray*) for a 50,000 period of the simulation. *Bottom*: Evolution of resonant argument θ_1.

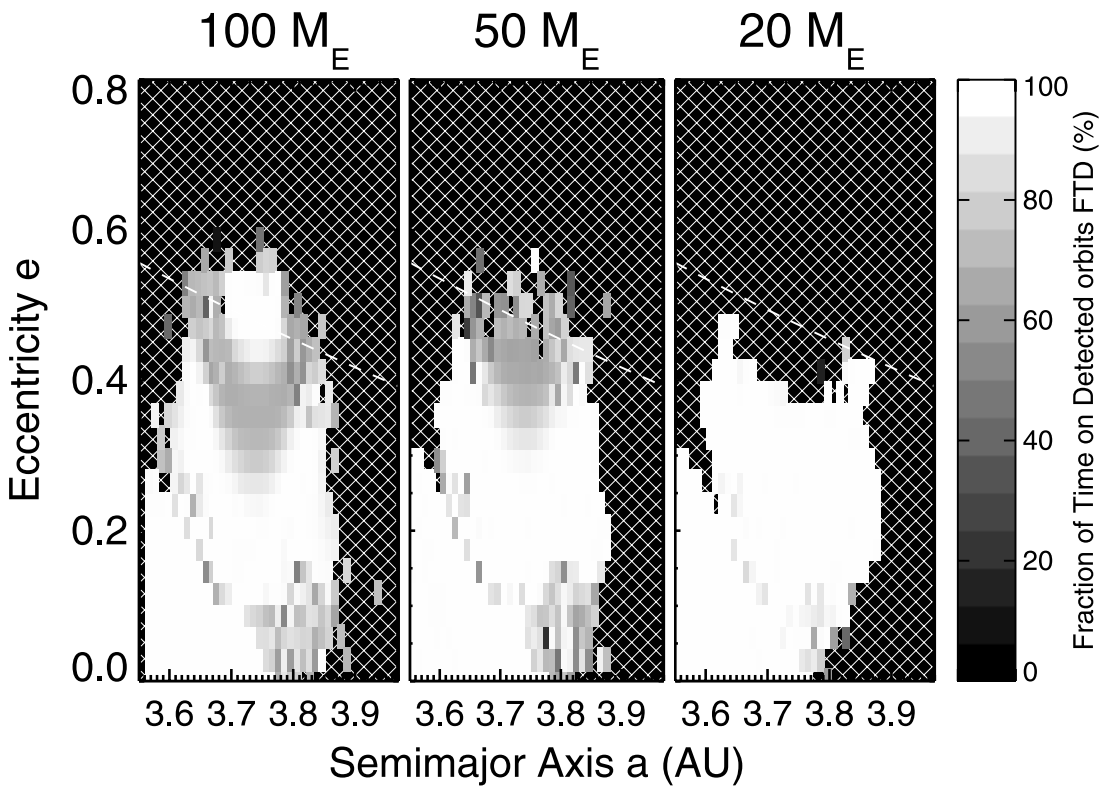

FIG. 4.— Stability and FTD of test planets in and near the 2 : 1 MMR with planet d (also called 2g : 1d), labeled by the test planet mass. The dashed line is the collision line with planet d. Formatted as in Fig. 1. [*See the electronic edition of the Journal for a color version of this figure*.]

the surrounding region of high FTD that extends from 2.6 to 2.85 AU, with e_g from 0.1 to 0.4. The lower FTD belt that separates these two regions has FTD ~ 0.7, so we cannot firmly exclude planets from that region. For smaller M_g, only the second region is available, although it reaches slightly higher e_g.

4.1.3. *The* 3g : 2d *MMR*

The 3g : 2d MMR is the most dramatic example of a stabilizing resonance. The entire resonant region is unstable to secular perturbations (see Fig. 1). Nonetheless, Figure 6 shows that there does exist a contiguous stable region here. Moreover, more than half of the resonant region has orbits that cross that of planet d. We find that all orbits across the collision line with planet d exhibit regular libration of the resonant angle $\theta_1 = 3\lambda_d - 2\lambda_g - \varpi_g$ about 0°, although none undergo apsidal libration. For the majority of cases below the collision line there is a preferential alignment of θ_1, θ_2, and $\varpi_g - \varpi_d$, but circulation does occur. The situation is similar for the three different values of M_g, although a larger fraction of systems exhibited stable resonant libration for lower M_g.

FTD values above the collision line are 0.5–0.8 for $M_g = 113\ M_\oplus$, 0.8–1 for $M_g = 50\ M_\oplus$, and 1 for $M_g = 20\ M_\oplus$. This suggests that the 3g : 2d MMR is unlikely to contain a planet more massive than $\sim 50\ M_\oplus$ above the collision line. However, just below the collision line FTD values are large for all masses so we cannot constrain M_g beyond the stability boundaries.

It is interesting that low-eccentricity test planets are unstable in this region. This appears to be due to short-term dynamical forcing from planet d, as the low-e_g region does not participate in the 3g : 2d MMR. Planet d's Hill sphere is very large, ~ 0.65 AU, such that any body exterior to 4.88 AU will cross planet d's orbit unless a favorable alignment (i.e., a resonance) prevents this. For a test planet starting at 4.5 AU, an eccentricity greater than 0.07 will bring the planet into the orbit-crossing region. Secular forcing from planet d is very strong in the region of the 3g : 2d MMR, so any planet not participating in the resonance will be quickly destabilized. For low-e_g orbits near, but not in, the 3g : 2d MMR, encounters between planets g and d can occur in less than two orbital periods of planet d.

4.2. *Unstable Resonances*—3g : 1d *and* 4g : 1d

4.2.1. *The 3g : 1d MMR*

The 3g : 1d MMR is not truly an unstable resonance, although Figure 7 shows that a large region of parameter space centered on the resonance (at ~ 2.88 AU)[5] is destabilized. However, a small range of test planets does show evidence of long-term stable libration of one of the three resonant arguments for the 3 : 1 MMR (see eq. [2]). This region is located at $a_g = 2.86$–2.89 AU and $e_g \leq 0.06$ (i.e., $e_g < e_d$). In these cases only one argument, θ_3, librates, whereas θ_1, θ_2, and $\varpi_g - \varpi_d$ all circulate. The eccentricities of planets g and d oscillate regularly within narrow ranges such that the FTD value of these resonant cases is low. In other words, a configuration with planet g in 3 : 1 resonance with planet d is observationally allowed, although the resonant region is narrow and restricted to very low eccentricities.

Figure 8 shows the evolution of two simulations, one in stable resonant libration and the other undergoing chaotic evolution including a time spent in resonance. In the stable case, the apses of planets d and g are circulating but θ_3 librates consistently with an amplitude of 60°. In contrast, the chaotic (and ultimately unstable) case undergoes resonant libration of θ_1 for 1.5 Myr, during which e_g remained confined in a relatively narrow band and $\varpi_g - \varpi_d$ librated about antialignment (see below). Once the resonance was

[5] The location of the resonance is shifted slightly from its nominal value of 2.83 AU by secular effects.

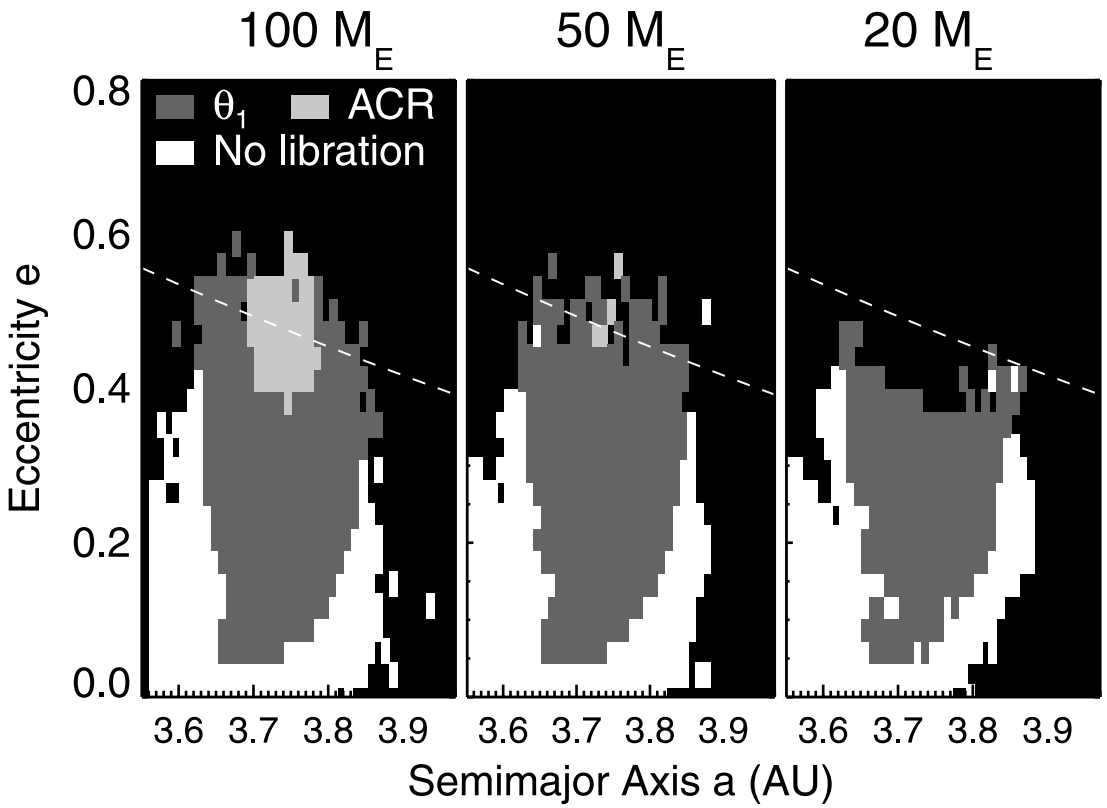

FIG. 5.—Stable zone of the 2g : 1d MMR, with colors that correspond to which resonant angles are librating. White indicates no resonant libration dark gray indicates libration of θ_2 and light gray libration of θ_1, θ_2, and $\varpi_g - \varpi_d$—this configuration is called the apsidal corotation resonance (ACR). Black areas are unstable. The dashed line is the collision line with planet d.

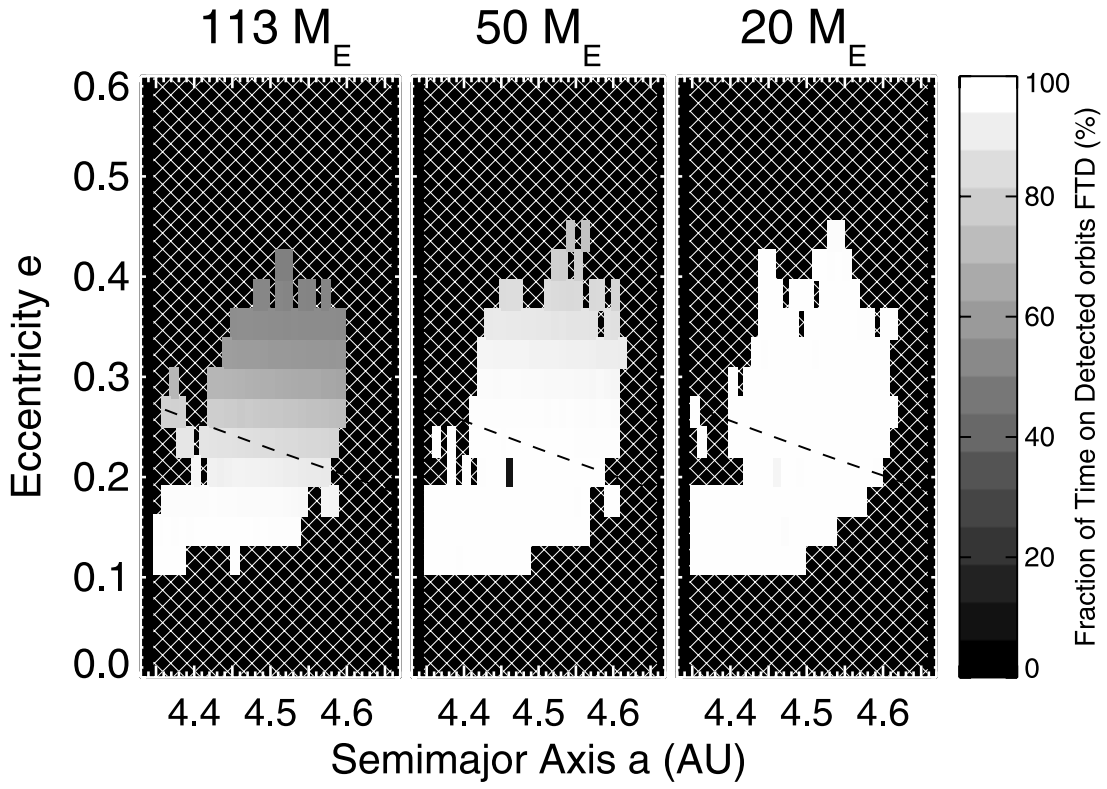

FIG. 6.—Stability and FTD of test planets in and near the 3 : 2 MMR with planet d (also called 3g : 2d), labeled by the test planet mass. The dashed line is the collision line with planet d. Formatted as in Fig. 1. [*See the electronic edition of the Journal for a color version of this figure.*]

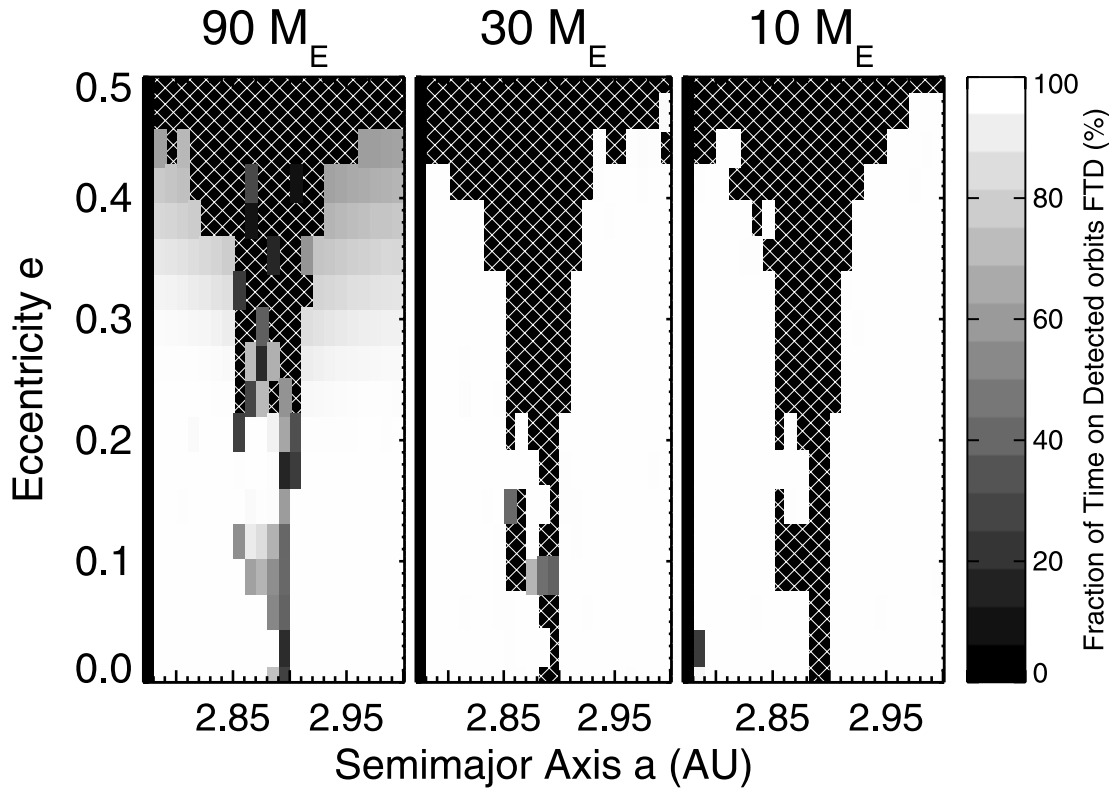

FIG. 7.—Stability and FTD of test planets in and near the 3 : 1 MMR with planet d (also called 3g : 1d), labeled by the test planet mass in Earth masses. Formatted as in Fig. 1. [*See the electronic edition of the Journal for a color version of this figure.*]

broken, e_g ranged from close to zero to above 0.5. At 3.2 Myr, planets g and d underwent a close encounter and the integration was stopped.

There exists a small "island" near the resonance at $a_g = 2.85$–2.88 AU with $e_g = 0.15$–0.2 which is stable for long timescales. This island is small but apparent for all three test planet masses and in all cases the island has high FTD values, i.e., test planets in this region do not strongly perturb the orbits of planets b–f. In this island, the longitudes of pericenter of planets d and g librate with low amplitude and eccentricities of both planets also oscillate with relatively low amplitudes. Thus, this island of low-amplitude apsidal libration has very high FTD values. There is

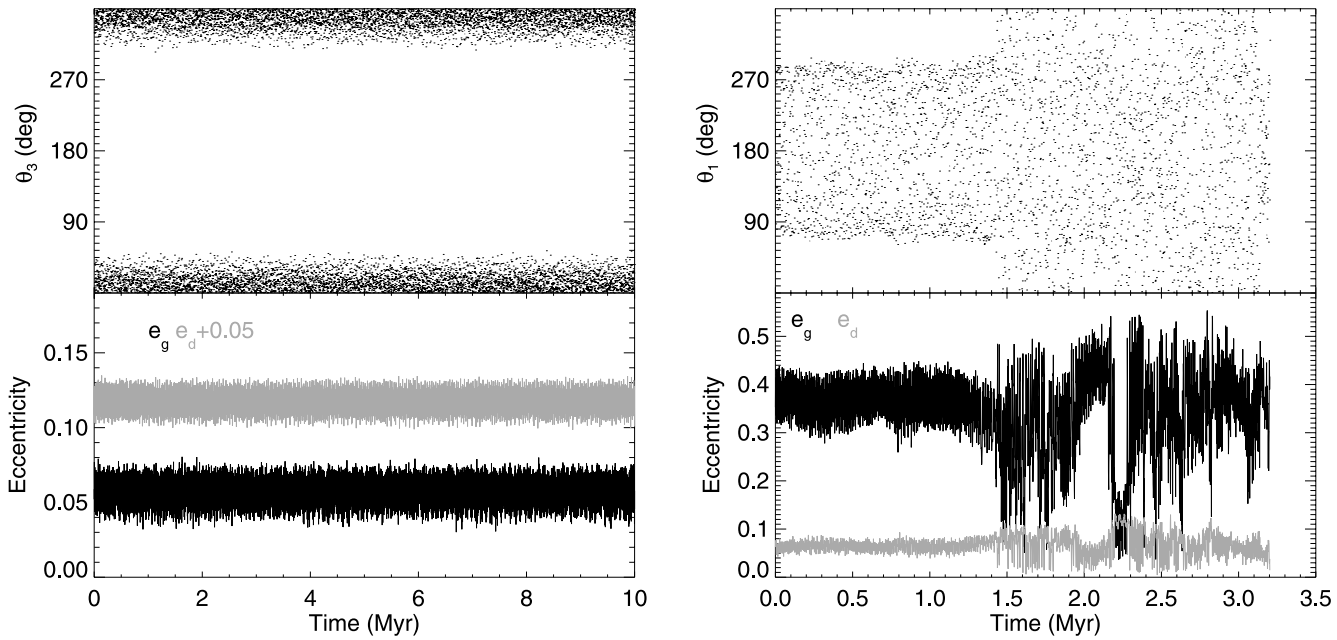

FIG. 8.—Evolution of two simulations for the 3g : 1d MMR, both with $M_g = 90\,M_\oplus$. *Left*: Evolution of θ_3 (see eq. [2]) and eccentricities e_g and e_d for a stable resonant planet (e_d shifted up by 0.05 for clarity). *Right*: Evolution of θ_1 and e_g, e_d for a chaotically evolving system in the resonant region. In this case, ϖ_g and ϖ_d started in an antialigned configuration and librated about 180° for the first ~1.5 Myr, while the system remained in resonance. This system went unstable after 3.2 Myr.

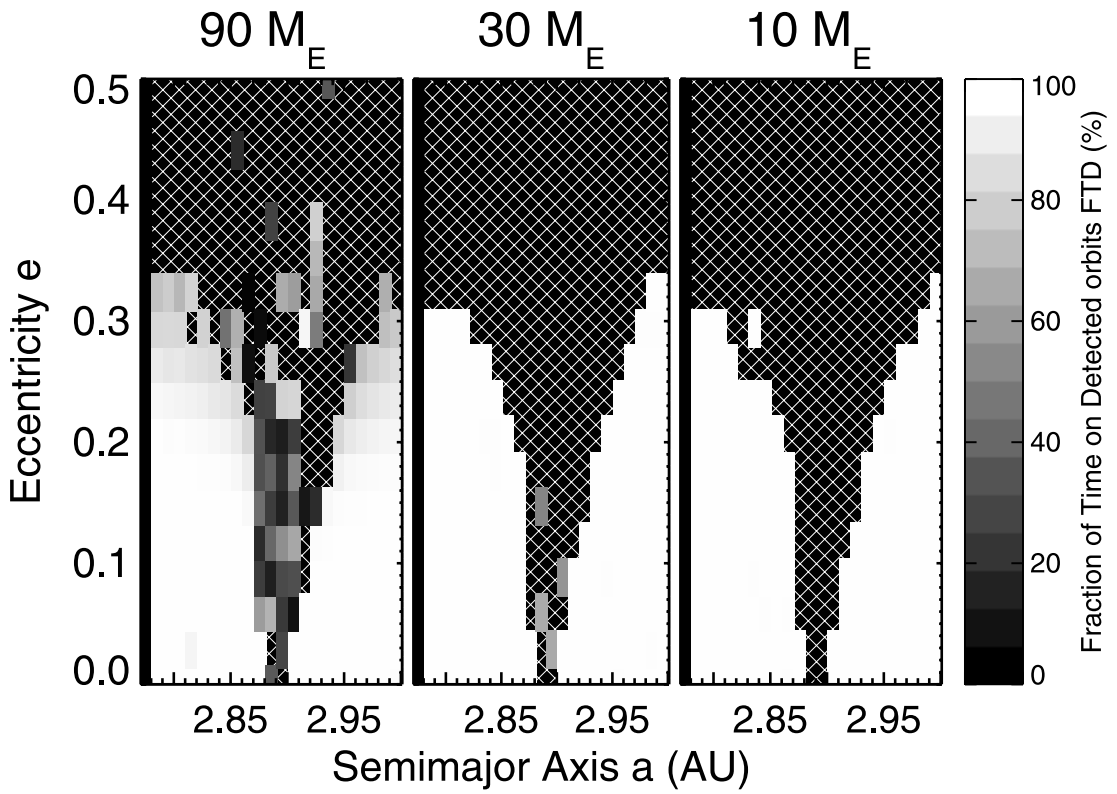

FIG. 9.—Stability and FTD of test planets in and near the 3 : 1 MMR with planet d (also called 3g : 1d), but with the longitudes of pericenter of planets g and d originally in antialignment (in Fig. 7 the apses are aligned). Again, panels are labeled by the test planet mass in Earth masses, and formatted as in Fig. 1. [*See the electronic edition of the Journal for a color version of this figure.*]

another region in Figure 7 which exhibits low-amplitude apsidal libration, with $a > 2.88$ AU and $e \sim 0.06$ (note that $e_d = 0.063$). This region is not distinct from surrounding orbits in terms of the FTD value; nonetheless it is strongly localized. It is interesting that this libration is so strong on one side of the resonance (i.e., at orbital period ratios with planet d of less than 3 : 1) and nonexistent on the other side of the resonance.

Test planets near the resonant region ($a_g = 2.86$–2.89 AU, $e_g \leq 0.06$) or apsidal-libration island ($a_g = 2.85$–2.88 AU, $e_g = 0.15$–0.2) may undergo temporary capture into the 3g : 1d resonance, i.e., temporary libration of one or more resonant arguments. However, in these cases the evolution of the system is typically chaotic such that resonant libration does not last for long times. The majority of these cases are unstable on the 10 Myr integration period, especially for smaller test planet masses M_g. For larger M_g, stable cases have small FTD values and so are observationally unlikely. In addition, we expect such cases to be unstable on longer timescales given the chaotic evolution of the system.

FTD values at large e_g are a function of M_g (see Fig. 7), as a more massive eccentric planet will impart larger perturbations on the other planets in the system. Note that these regions do not undergo resonant or apsidal libration.

We reran the same cases with the apses of planets g and d antialigned rather than aligned; Figure 9 summarizes the outcome. For antialigned apses we see the same instability of planets in the resonant region, but no island of apsidal libration was apparent. There also existed a few cases undergoing stable resonant libration of θ_3 in the same region as the aligned case ($a_g = 2.86$–2.89 AU), but only for initial $e_g = 0$. The only other test planets that underwent resonant libration were for $M_g = 90\ M_\oplus$ at higher eccentricities. As before, these cases evolve chaotically and have high FTD values. Such orbits are unstable for smaller M_g and likely unstable on longer timescales for $M_g = 90\ M_\oplus$.

The stability limits far from resonance differ between the aligned and antialigned simulations. In particular, the edges of the resonance occur at lower eccentricities for the antialigned case (at $e_g = 0.3$–0.35 rather than 0.45–0.5). This appears to be due to stronger secular forcing for the cases which are initially antialigned. In other words, antialigned test planets start the simulations in a phase of eccentricity growth and aligned planets start in a phase of eccentricity decline. Thus, the long-term median eccentricity of planet g in an antialigned configuration with planet d is significantly larger than the eccentricity of planet g starting in an aligned configuration. Higher eccentricities lead to closer encounters with other planets, which is the key factor in determining the stability of a planetary system (e.g., Marchal & Bozis 1982; Gladman 1993; Barnes & Greenberg 2006, 2007). Therefore, for a given starting eccentricity, a planet in an antialigned configuration will have a higher average eccentricity than for an aligned configuration—this higher eccentricity will bring the antialigned case closer to instability. So, although the stability limit for aligned and antialigned cases has the same time-averaged eccentricity, this limit occurs for smaller *starting* eccentricities for the antialigned configuration. It is therefore important to note that the initial eccentricity is not necessarily a good measure of the typical eccentricity during an integration, especially when comparing systematically different orbital angles.

4.2.2. *The* 4g : 1d *MMR*

The 4 : 1 MMR with planet d is strongly dependent on M_g (see Fig. 10). For both $M_g = 80\ M_\oplus$ and $40\ M_\oplus$, the outskirts of the resonance at high FTD values show the same structure. However,

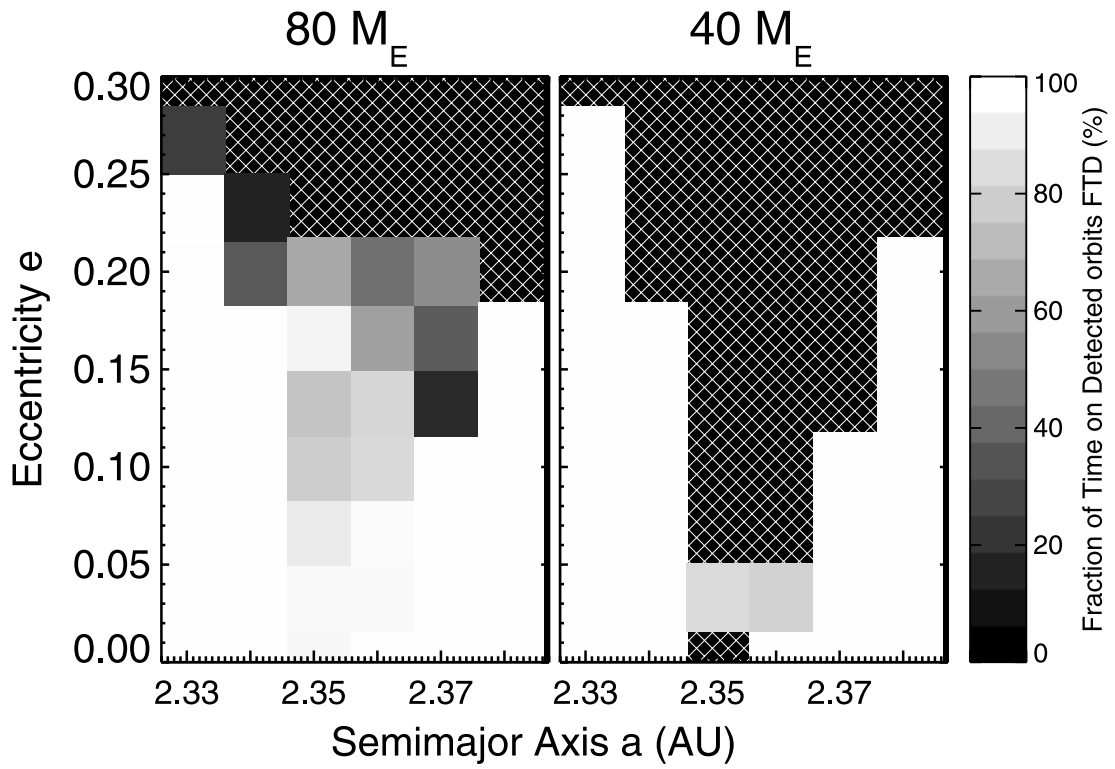

FIG. 10.— Stability and FTD of test planets in and near the 4 : 1 MMR with planet d (also called 4g : 1d), labeled by the test planet mass. Formatted as in Fig. 1. [*See the electronic edition of the Journal for a color version of this figure.*]

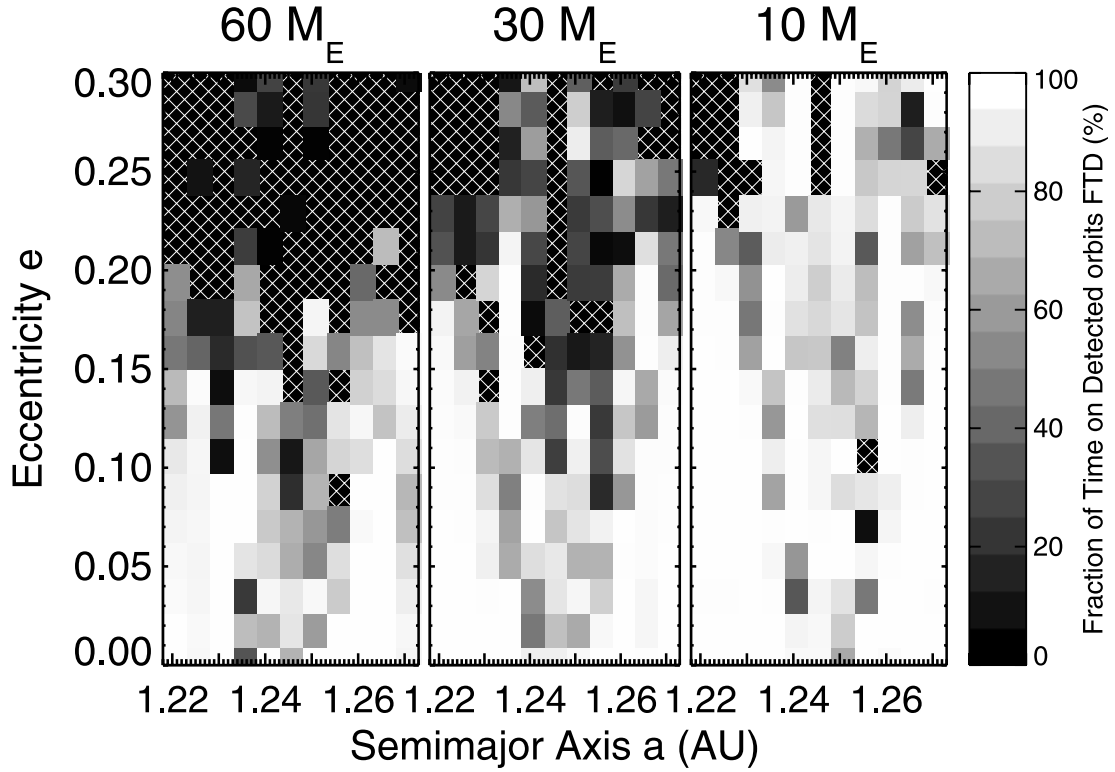

FIG. 11.— Stability and FTD of test planets in and near the 1 : 2 MMR with planet f (also called 1f : 2g), labeled by the test planet mass. Formatted as in Fig. 1. [*See the electronic edition of the Journal for a color version of this figure.*]

the heart of the resonance, at 2.35–2.36 AU, is populated with lower FTD planets for $M_g = 80\ M_\oplus$ and is empty for $M_g = 40\ M_\oplus$. Planets in this region undergo chaotic and temporary capture into resonant libration. However, the resonance never persists for more than a few Myr. For $M_g = 40\ M_\oplus$ we see the same phenomenon but the timescale for such planets to become dynamically unstable is shorter, such that very few survive for 10 Myr. We suspect that this chaotic region will be cleared out for $M_g = 80\ M_\oplus$ on timescales that are somewhat longer, but still short compared with the lifetime of the system. Thus, we do not expect any planets to exist in the 4g : 1d MMR.

4.3. *Neutral Resonances*—2f : 1g, 3f : 1g, *and* 5g : 2d

4.3.1. *The* 2f : 1g *MMR*

The 2f : 1g MMR is located at ~1.24 AU. Figure 11 shows a lot of substructure within the resonance, with significant variations in FTD and stability between neighboring test planets. We believe these variations are caused by a combination of secular effects and sparse sampling. Nonetheless, we see a clear trend of higher FTD and greater stability for lower M_g.

For $M_g > 10\ M_\oplus$ only a very limited sample of test planets show evidence for libration of 2f : 1g resonant angles. Indeed, for $M_g = 30$ and $60\ M_\oplus$ the only region which exhibits resonant libration is at $a_g = 1.24$ and 1.25 AU, and $e_g = 0.26$–0.30. In this region libration of $\theta_2 = 2\lambda_g - \lambda_f - \varpi_f$ occurs but with varying amplitudes and in a chaotic fashion with occasional circulation. However, the median FTD value of these resonant planets is only 0.1 ($M_g = 60\ M_\oplus$) and 0.37 ($M_g = 30\ M_\oplus$). A large range of parameter space exhibits temporary libration of resonance angles but no long-term resonance. This region is centered at 1.24–1.25 with somewhat smaller eccentricities, and has small FTD values. In contrast, for $M_g = 10\ M_\oplus$, several regions exhibit stable resonant libration. Resonant orbits tend to correlate with high FTD values in the V-shaped region and tend to lie at the edges at $a_g =$ 1.24 and 1.26 AU.

Figure 12 shows the evolution of resonant angles θ_1 and θ_2 for two simulations, both starting with $a_g = 1.251$ AU and $e_g = 0.282$, but with $M_g = 60$ and $10\ M_\oplus$. For $M_g = 60\ M_\oplus$, θ_2 librates about 0° in irregular fashion with occasional circulation, and θ_2 circulates. For $M_g = 10\ M_\oplus$ the situation is quite different: θ_1 librates steadily about 75° with an amplitude of 30°, and θ_2 librates about 315° with an amplitude of ~90° but with occasional circulation.[6] The contrast between the two cases is remarkable and leads us to the conclusion that it is very unlikely for a planet with $M_g \gtrsim 20\ M_\oplus$ to exist in the 2f : 1g MMR.

4.3.2. *The* 3f : 1g *MMR*

The 3f : 1g MMR lies at 1.63 AU. Figure 13 shows a clear trend between lower FTD in this region and larger M_g. Thus, the 3f : 1g MMR is unlikely to contain a planet more massive than ~30 $M_\oplus$. The mean (median) values of the FTD for simulations with $a_g = 1.633$ AU are 0.49 (0.59) for $M_g = 68\ M_\oplus$, 0.69 (0.80) for $M_g = 30\ M_\oplus$, and 0.97 (0.98) for $M_g = 10\ M_\oplus$.

None of the planets with $a_g = 1.633$ AU in Figure 13 (the central "column" of a_g values) stay in resonance for long timescales. Resonant angles librate temporarily in many cases before switching to circulation, and sometimes back to libration in irregular fashion. Despite this chaotic behavior, most of these cases appear to be stable for 10 Myr, without undergoing close approaches with planet f. Many of the simulations with $a_g = 1.628$ and 1.638 AU in Figure 13 exhibited a period of apsidal libration between planets f and g. As for the resonant cases, periods of circulation and libration were often chaotically interspersed, but the simulations were nonetheless stable and with high FTD values. For smaller M_g, there exist fewer planets which exhibit temporary resonant libration, but the region of temporary apsidal libration is expanded. For the most part, regions of low FTD correspond to chaotic zones and high FTD correspond to temporary apsidal libration.

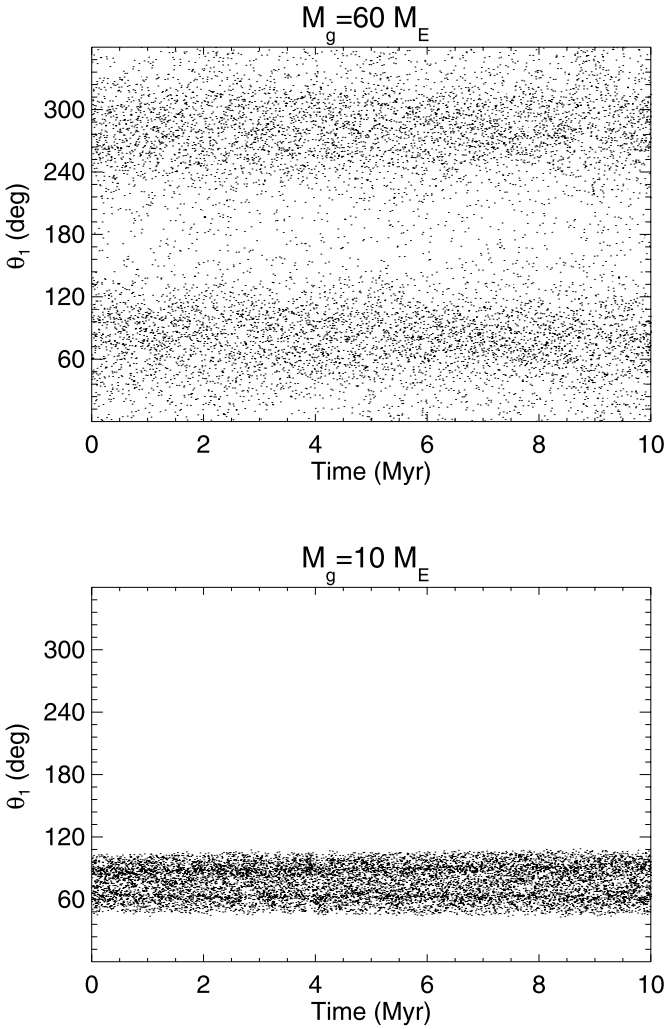

FIG. 12.—Evolution of resonant argument θ_1 for two simulations of the 2f : 1g MMR. For the top panel, $M_g = 60\ M_\oplus$ and for the bottom panel $M_g = 10\ M_\oplus$.

4.3.3. *The* 5g : 2d *MMR*

Figure 14 shows the stability and FTD of planet g in and near the 5 : 2 resonance with planet d. The structure of the phase space is quite simple in this case and can be broken into four regions. The first region, represented as high FTD areas at $e_g < 0.07$, undergoes regular apsidal libration but is not in resonance. The second, smaller region also has high FTD values and is located at $a_g \approx$ 3.20–3.225 AU and $e_g = 0.25$–0.4. This region is wider for $M_g =$ 50 $M_\oplus$ than for 95 $M_\oplus$, but the characteristics are the same for the two values of M_g: this zone undergoes stable libration of all four resonant arguments, as well as apsidal libration. This region is therefore in the apsidal corotation resonance, also seen for large M_g in the 2g : 1d MMR. The third region comprises the low FTD region centered on the resonant region, at slightly smaller a_g and e_g. This chaotic region is where test planets may be temporarily captured into resonance or apsidal libration but the evolution is

[6] It is uncommon for resonant angles to librate about values other than 0° or 180° but can happen in some circumstances (e.g., Zhou & Sun 2003).

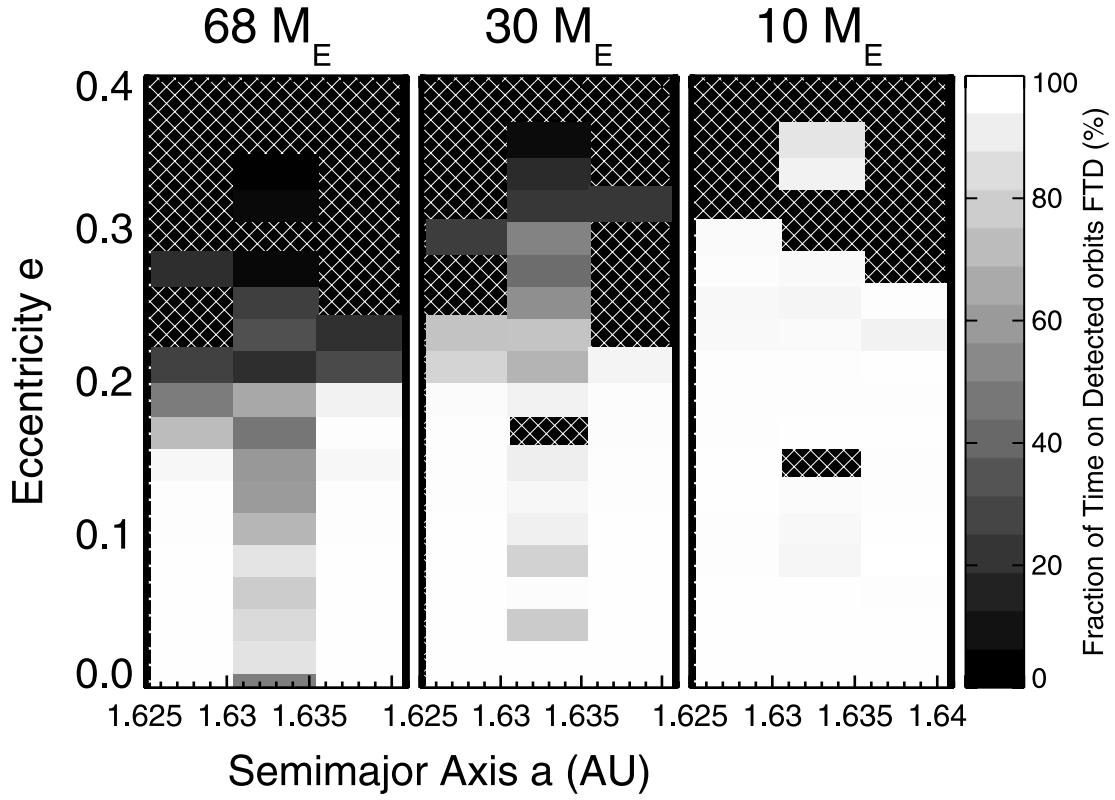

FIG. 13.— Stability and FTD of test planets in and near the 1 : 3 MMR with planet f (also called 1f : 3g), labeled by the test planet mass. Formatted as in Fig. 1. [*See the electronic edition of the Journal for a color version of this figure.*]

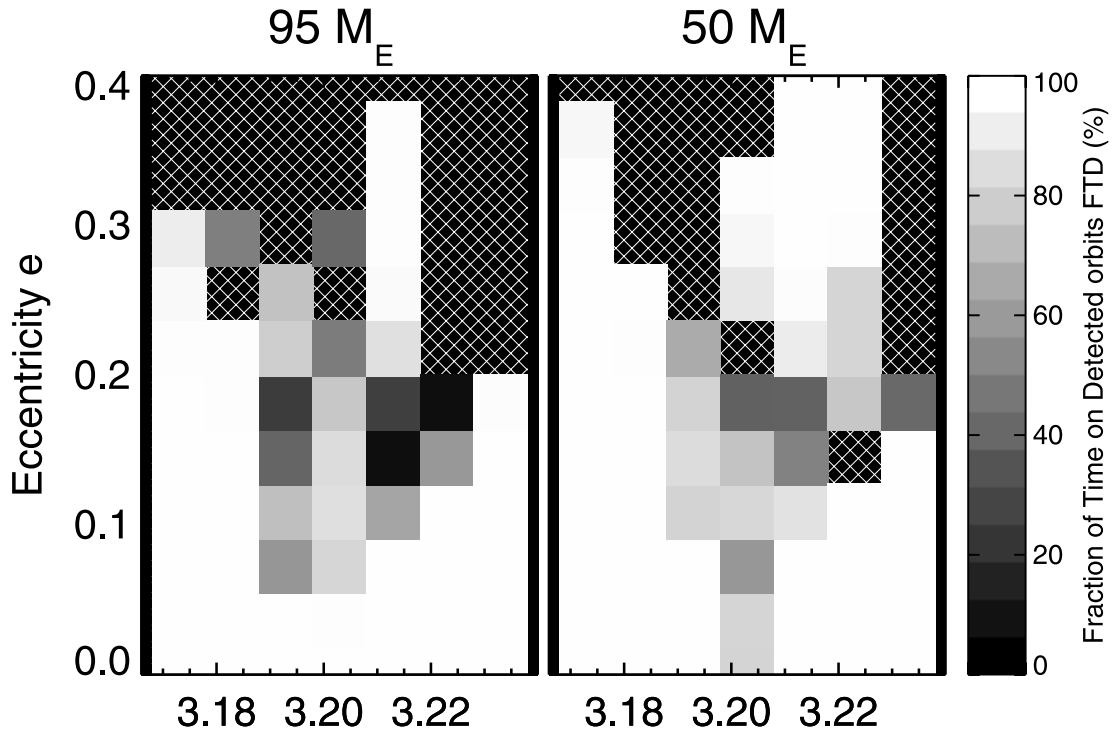

FIG. 14.— Stability and FTD of test planets in and near the 5 : 2 MMR with planet d (also called 5g : 2d), labeled by the test planet mass. Formatted as in Fig. 1. [*See the electronic edition of the Journal for a color version of this figure.*]

chaotic and the resonance is short-lived. The fourth and final region includes the high-FTD areas at the edges of our sampled zone, at $e_g \gtrsim 0.1$. This region does not participate in the resonance or apsidal libration.

For planet g to be located in the 5g : 2d MMR, it must be localized in both a_g and e_g. It must reside at $a_g \sim 3.21$ AU with $e_g \sim 0.3$; this resonant region is wider for lower M_g. The surrounding region is unlikely to host a massive planet given the low FTD values. But for low e_g, the entire region is allowed and apsidal libration is preferred.

4.4. *The* 3c : 1b *MMR*

Planets b and c lie very close to the 3 : 1 MMR (Marcy et al. 2002; Ji et al. 2003), but Fischer et al. (2008) note that the resonant arguments are circulating rather than librating. In other words, planets b and c are not in resonance. Since an additional planet g can affect the mean motions of other planets in the system, we calculated resonant angles of planets b and c for all of our stable six-planet simulations. We find that, for our chosen configuration of known planets b–f, there are no cases in which planet g causes the resonant angles of planets b and c to librate. Thus, we conclude that the only way for planets b and c to truly be in a resonance is if our assumed orbital parameters for planets b–f are incorrect, which is certainly possible given the observational uncertainties.

5. MULTIPLE PLANETS IN THE STABLE ZONE

Given the width of the stable zone between planets f and d, more than one additional planet could exist in the region. We ran additional simulations including multiple planets in the stable zone. For simplicity, we chose a fixed mass of 50 $M_\oplus$ for all additional planets. Planets were spaced such that their closest approach distances (perihelion q_1 vs. aphelion Q_2) were separated by a fixed number Δ of mutual Hill radii R_H, where $R_H = 0.5(a_1 + a_2)\left[(M_1 + M_2)/3M_\star\right]^{1/3}$ (Chambers et al. (1996) and subscripts 1 and 2 refer to adjacent planets. We ran simulations with planets spaced by $\Delta = (5–14.5)R_H$ in increments of 0.5 R_H, with five simulations for each separation with eccentricities chosen randomly to be less than 0.05, for a total of 100 simulations. The number of additional planets varied with the planet spacing, from five planets in the stable zone for $\Delta = 5$ to two for $\Delta = 14.5$. No cases with five extra planets was stable, and only one case with four extra planets survived for 10 Myr and the evolution of that case was chaotic. However, roughly 40% (11/28) of cases with three additional planets survived. Typical configurations for stable simulations with three planets contained planets at 1.1–1.2 AU, 1.6–1.9 AU, and 2.5–2.9 AU. The vast majority (43/45 = 96%) of systems with two extra planets were stable for 10 Myr. These contained additional planets at 1.3–1.6 and 2.2–3.3 AU. All stable cases had very high FTD values (>97%).

6. PLANETS EXTERIOR TO PLANET d

Figure 15 shows the survival time of test particles beyond planet d as a function of their semimajor axis. As expected, there is a several AU-wide region just beyond planet d in which low-mass planets are unstable. In this region particles' eccentricities are quickly excited to values that cause them to cross the orbit of planet d, resulting in close encounters and ejections. Farther out, there exists a narrow contiguous region of stability from 8.6 to 9 AU, which is roughly bounded by the 4 : 7 and 1 : 2 MMRs with planet d. This stable region is the only difference between our results and those of Rivera & Haghighipour (2007), who also mapped this outer region using test particles. The difference arises

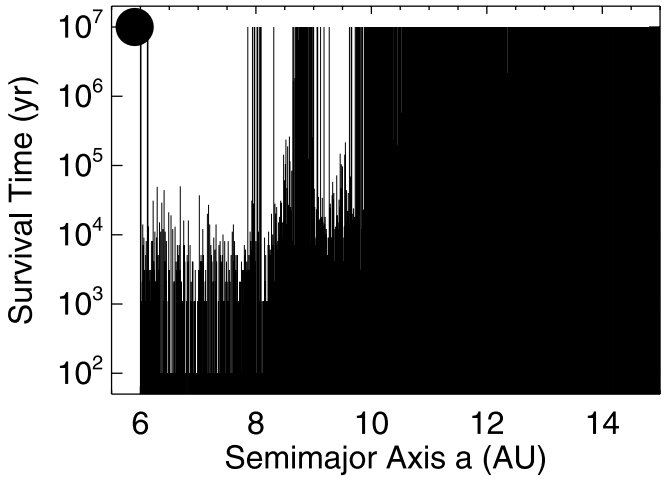

FIG. 15.— Survival time of test particles exterior to planet d at 5.9 AU (*black circle*). Test particles extended to 30 AU; all past 15 AU were stable.

from the significant decrease in the best-fit eccentricity of planet d, from 0.244 to 0.063.

A plateau of stability starts at 9.7 AU and extends continuously to 30 AU, except for a very narrow region of instability at the 3 : 1 MMR with planet d at 12.3 AU. Thus, the innermost planet beyond planet d is likely to be located at 10 AU or beyond, although it could inhabit the stable zone at 8.6–9 AU.

7. CONCLUSIONS

We have mapped out the region in 55 Cancri where an additional planet g might exist. There is a broad region of stability between known planets f and d that could contain a ~Saturn-mass planet (Fig. 1). Since observations rule out a very massive planet, our simulations suggest that the region could easily support two or possibly even three additional planets. In addition, one or more outer planets could be present in the system beyond about 10 AU. However, such distant planets would not be detectable for many years.

We examined eight mean motion resonances in detail (see Table 2). For two of these, 3f : 1g (i.e., the 1 : 3 MMR between planet f and hypothetical planet g) and 4g : 1d, there was no stable region that exhibited regular libration of resonant arguments. Therefore, these resonances cannot contain planets in the mass range that we explored. Given the very low FTD values, the 2f : 1g MMR is unlikely to contain a resonant planet more massive than ~20 $M_\oplus$. Two other MMRs, 3g : 1d and 5g : 2d, may contain a stable, high-FTD resonant planet but the location of the MMRs is constrained to a very small region of (a_g, e_g) space which is surrounded by a chaotic region. Finally, three MMRs, 3f : 2g, 2g : 1d, and 3g : 2d, have a stabilizing influence and may contain planets near or even across the collision line with planet f or d. Each of these MMRs contains broad regions of stable libration of resonant angles, although the locations of low-FTD libration can vary with M_g. We can therefore only weakly constrain the presence of an additional planet in one of these resonances.

The region between planets f and d contains many MMRs which display a wide range of behavior. In addition to stable and unstable resonances, the behavior of resonant arguments is also diverse. In some regions we would expect all resonant angles to librate regularly, but in others only some librate. In two instances, planet g could be in the apsidal corotation resonance (Beaugé & Michtchenko 2003; Ferraz-Mello et al. 2003): for large M_g in the 2g : 1d MMR at the g–d collision line (see Fig. 5), or in 5g : 2d MMR (Fig. 14). Moreover, we also see cases of "asymmetric"

libration in which the equilibrium angle is neither 0° or 180° (see Fig. 8). Even if there are no additional planets in the f–d gap, there could be an asteroid belt in which this diverse and exotic dynamical behavior is on display.

55 Cancri is a critical test of the "packed planetary systems" (PPS) hypothesis, which asserts that any large contiguous stable region should contain a planet (BR04; RB05; Raymond et al. 2006; Barnes et al. 2008). To date, two planets have been discovered in the three stable zones mapped out by BR04 and RB05 (in HD 74156 and 55 Cnc). Given the width of the stable zone between planets f and d, PPS indicates that at least one, and possibly two or three, more planet(s) should exist in 55 Cancri. We look forward to further observations of the system that may find such planets, or perhaps show evidence of their absence. Our results may be used to guide observers searching for planet g and beyond.

We are indebted to Google for allowing us to run these simulations on their machines. We thank the anonymous referee for pointing out several important issues that improved the paper. S. N. R. was supported by an appointment to the NASA Postdoctoral Program at the University of Colorado Astrobiology Center, administered by Oak Ridge Associated Universities through a contract with NASA. R. B. acknowledges support from NASA's PG&G grant NNG05GH65G and NASA Terrestrial Planet Finder Foundation Science grant 811073.02.07.01.15.

REFERENCES

Barnes, R., Goździewski, K., & Raymond, S. N. 2008, ApJ, 680, L57
Barnes, R., & Greenberg, R. 2006, ApJ, 652, L53
———. 2007, ApJ, 665, L67
Barnes, R., & Quinn, T. 2004, ApJ, 611, 494
Barnes, R., & Raymond, S. N. 2004, ApJ, 617, 569 (BR04))
Bean, J. L., McArthur, B. E., Benedict, G. F., & Armstrong, A. 2008, ApJ, 672, 1202
Beaugé, C., & Michtchenko, T. A. 2003, MNRAS, 341, 760
Butler, R. P., Marcy, G. W., Williams, E., Hauser, H., & Shirts, P. 1997, ApJ, 474, L115
Chambers, J. E. 1999, MNRAS, 304, 793
Chambers, J. E., Wetherill, G. W., & Boss, A. P. 1996, Icarus, 119, 261
Cincotta, P. M., & Simó, C. 2000, A&AS, 147, 205
Ferraz-Mello, S., Beaugé, C., & Michtchenko, T. A. 2003, Celest. Mech. Dyn. Astron., 87, 99
Fischer, D. A., et al. 2008, ApJ, 675, 790
Froeschlé, C., Lega, E., & Gonczi, R. 1997, Celest. Mech. Dyn. Astron., 67, 41
Gladman, B. 1993, Icarus, 106, 247
Goździewski, K., & Maciejewski, A. J. 2001, ApJ, 653, L81
Ji, J., Kinoshita, H., Liu, L., & Li, G. 2003, ApJ, 585, L139
Jones, B. W., Underwood, D. R., & Sleep, P. N. 2005, ApJ, 622, 1091
Laskar, J. 1996, Celest. Mech. Dyn. Astron., 64, 115
Lee, M. H., & Peale, S. J. 2002, ApJ, 567, 596
Marchal, C., & Bozis, G. 1982, Celest. Mech. Dyn. Astron., 26, 311
Marcy, G. W., Butler, R. P., Fischer, D. A., Laughlin, G., Vogt, S. S., Henry, G. W., & Pourbaix, D. 2002, ApJ, 581, 1375
Marzari, F., Scholl, H., & Tricarico, P. 2006, A&A, 453, 341
McArthur, B. E., et al. 2004, ApJ, 614, L81
Michtchenko, T. A., Beaugé, C., & Ferraz-Mello, S. 2008, MNRAS, 387, 747
Morbidelli, A., Tsiganis, K., Crida, A., Levison, H. F., & Gomes, R. 2007, AJ, 134, 1790
Murray, C. D., & Dermott, S. F. 1999, Solar System Dynamics (Cambridge: Cambridge Univ. Press)
Raymond, S. N., & Barnes, R. 2005, ApJ, 619, 549 (RB05)
Raymond, S. N., Barnes, R., Armitage, P. J., & Gorelick, N. 2008, ApJ, 687, L107
Raymond, S. N., Barnes, R., & Kaib, N. A. 2006, ApJ, 644, 1223
Rivera, E., & Haghighipour, N. 2007, MNRAS, 374, 599
Sándor, Z., Süli, Á., Érdi, B., Pilat-Lohinger, E., & Dvorak, R. 2007, MNRAS, 375, 1495
Šidlichovský, M., & Gerlach, E. 2008, in IAU Symp., 249, Exoplanets: Detection, Formation, and Dynamics, ed. Y.-S. Sun & S. Ferraz-Mello (Cambridge: Cambridge Univ. Press), 479
Snellgrove, M. D., Papaloizou, J. C. B., & Nelson, R. P. 2001, A&A, 374, 1092
Valenti, J. A., & Fischer, D. A. 2005, ApJS, 159, 141
Wisdom, J., & Holman, M. 1991, AJ, 102, 1528
Zhou, J.-L., & Sun, Y.-S. 2003, ApJ, 598, 1290